Int. J. Electrochem. Sci., 15 **(2020)** 6778 – 6789, doi: 10.20964/2020.07.25

International Journal of
ELECTROCHEMICAL
SCIENCE
www.electrochemsci.org

Au@Pt Nanoparticles Embedded in N-doped Graphene as sensor for Determination of Catechin

Shaoping Feng[1,2,3], *Shaoqin Hu*[1,2], *Xianlan Chen*[1,2,*], *Guowei Zhang*[1,2,*], *Guiyang Liu*[1,2,*], *Wei Liu*[1,2]

[1] College of Science, Honghe University, Mengzi, 661199, Yunnan, P.R.China
[2] Local Characteristic Resource Utilization and New Materials Key Laboratory of Universities in Yunnan, Honghe University, Mengzi, 661199, Yunnan, China
[3] School of Metallurgical and Ecological Engineering, University of Science and Technology Beijing, Beijing 100083, China
[*]E-mail: 13489086418@163.com , shaopingfeng@126.com, 47225018@qq.com, alios@126.com

Received: 21 February 2020 / *Accepted:* 24 April 2020 / *Published:* 10 June 2020

In this study, N-doped grapheme (NG) was synthesized by a hydrothermal method with graphemes oxide (GO) as raw material, melamine ($C_3H_6N_6$) as reductant and nitrogen source. Results indicated that the nitrogen atoms have been effectively embedded into graphene when the composition mass ratio of GO:$C_3H_6N_6$ was 3:1. After that, the NG was saturated with Au@Pt core-shell nanoparticles (Au@Pt NPs), which prepared by seed-mediated growth method, to obtain N-doped Au@Pt core-shell nanoparticles (NG-Au@Pt NPs). Then, the NG-Au@Pt NPs was dropped on Au electrode to construct an electrochemical sensor (NG-Au@Pt NPs/Au electrode) for sensing catechin. The electrochemical behaviors on modified electrode of catechin were investigated in detail at desired different conditions. The electrochemical sensor for catechin determination showed an excellent response and exhibited a wide linear range of 1.0×10^{-7}-4.5×10^{-5} M with the detection limit of 2.85×10^{-9} M. The recovery range and the precision relative standard deviation were 99.94-101.5% and 0.06-1.5% for determination of catechin in teas, respectively, indicating that the proposed method was expeditious and reasonable for catechin determination.

Keywords: N-doped graphene; Au@AuPt NPs; Catechin; Electrochemical sensor

1. INTRODUCTION

Tea is considered as an indispensable nutraceutical and has become more and more important in our daily life because of its numerous beneficial properties, including anti-bacterial, anti-oxidative, anti-mutagenic and anti-cancer effects [1]. Tea contained about 4000 bioactive compounds, in which catechin is one of the important constituents [2]. Catechin exsisted in tea has attracted extensive attention due to anti-oxidative activity, which can expeditiously reduce free radicals

[3]. In addition, the results of clinical research show that catechin can bring forth a positive effect on disease prevention and reduced the risk of disease, such as cardiovascular diseases, neurodegenerative diseases and certain cancers [3, 4]. In view of several biological activities, catechin is a potential candidate for therapeutic agents. Therefore, it is essential and desirable to develop an efficient and sensitive method for detection of catechin, which can illuminate its properties and physiological function.

Many detection techniques have been carried out to analyze catechins, such as capillary electrophoresis (CE) [5], thin-layer chromatography (TLC) [6], LC/MS [7, 8], HPLC [9, 10] and electrochemical analysis [11, 12]. Among these approaches, the electrochemical analysis has several advantages including time savings, high-sensitivity and low-cost [13]. El-Hady et al. successfully constructed HP-β-CD incorporated carbon paste modified electrode and used to determinate of catechin in many commercial drinking samples and biological fluids [14]. Anna Jarosz-Wilkołazka et al. reported a graphite electrode modified with laccase and applied for determination of catechin [15]. Yang et al. investigated the electrochemical properties of catechin at SWNTs-CTAB/GCE and indicated that the modified electrode could be used to detect catechin with excellent stability and reproducibility [11].

Recently, graphene and its derivatives, especially nitrogen-doped Graphene (NG) and graphene oxide (GO), have attracted considerable attention in the design of electrodes due to their excellent properties [16, 17]. In this article, the preparation and application of N-doped graphene/Au@Pt core-shell nanomaterials modified electrodes (NG-Au@Pt NPs/Au electrode) as an electrochemical sensor for the determination of catechin were proposed. Experimental results showed that the proposed method was successfully used to determination of catechin in tea samples with excellent sensitivity and stability.

2. EXPERIMENT

2.1 Reagents

$HAuCl_4$, $NaBH_4$, H_2PtCl_6, catechin and melamine ($C_3H_6N_6$) were purchased from Sinopharm Chemical Reagent Co. Ltd. (Shanghai, China). Graphite powder (99.95%, 325 mesh) was purchased from Alfa Aesar Co. Ltd. (Tianjin, China). The desired working solutions were obtained by diluting the stock solution with ultra-pure water and phosphate buffer solution (PBS, NaH_2PO_4-Na_2HPO_4). All the other chemicals were of AR grade and used without further purification.

2.2 Instruments and characterizations

UV-vis spectra (Perkin-Elmer Lambda 900 USA) was used to obtain UV-vis absorption spectra of Au and Au@Pt NPs. X-ray diffraction (XRD, X'pert, Philips, Holland) and XPS (Thermal Scientific K-Alpha XPS spectrometer) were used to ascertain the phase structures and atomic composition ratio of the samples, respectively. SEM (Nova Nano SEM 230, FEI, USA) and HRTEM

(Tecnai G2 F20 S-TWIN, 200 kV, FEI Company, USA) were employed to obtian the surface morphologies and microstructure of the materials.

Cyclic voltammetry (CV) and differential pulse voltammogram (DPV) were performed on electrochemical workstation (CHI 660C, Shanghai). The electrochemical cell consisted of a three electrode system with a bare Au electrode (3.0 mm in diameter) or modified working electrode as a working electrode, a platinum wire as a counter electrode and Ag/AgCl electrode as a reference electrode. PBS (0.20 M, pH=2.2) was added into the electrochemical cell and all the detection solutions were purged with N_2 for at least 15.0 min before measurements. All measurements were performed at room temperature.

2.3 Preparation of Au@Pt NPs

To obtain core-shell type nanoparticles of Au@Pt NPs, three steps were required. Au seeds were synthsized according to Frens' method firstly [18]. Then, 450 μL 1.0 mM H_2PtCl_6 and 660 μL ultra-pure water was dropped gradually into a conical beaker contained 2 mL Au seeds while stirring. The mixtures were cooled down to ca. 4.0 ˚C in an ice bath and stirred for 5.0 min. Finally, 220 μL 10.00 mM $NaBH_4$ was added gradually into the solution and stirred for another 30.0 min. The color of the deep purple solution changed to black, which suggests that the Au@Pt NPs formed. The UV-vis spectra, XRD and TEM of Au@Pt NPs were shown in Fig. 1.

2.4 Preparation of NG and NG-Au@Pt NPs

In this experiment, GO was synthesized by Hummers method [19]. NG was synthesized by a hydrothermal method with GO as raw material, $C_3H_6N_6$ as reductant and nitrogen source. When ethylene glycol was used as the solvent, GO and $C_3H_6N_6$ with the mass ratio ratio of 1:3 were put into a high-pressure reaction kettle and heated at 180 °C for 3h under stirring to prepare the NG. The SEM, TEM and XPS of NG were shown in Fig. 2 and Fig. 3, respectively. Finally, Au@Pt NPs (30 mL) and NG (10 mL) were mixed and stirred in ice bath for 3 h until to obtain NG-Au@Pt NPs with uniform dispersion.

2.5 Preparation of electrode and analytical procedure

The bare Au electrode was polished with alumina powders (1.0, 0.3 and 0.05 μm) in series. Afterward, the electrode was ultrasonicated in 50% nitric acid, ethanol and water successively about 5 min after each polishing, respectively. The electrode was dried under pure N_2. Then, 5.0 μL the NG-Au@Pt NPs was uniformly dropped on Au electrode surface, and a film coated electrode of NG-Au@Pt NPs/Au electrode was obtained after drying with infrared lamp. Similarly, the NG/Au electrode and Au@Pt NPs/Au electrode as compared were fabricated. The modified electrode was renewed after each measurement by a multi-circle potential scan in the potential range (0.0-0.8 V) in a blank PBS (pH = 2.2) until the background CV curve was not changed.

3. RESULTS AND DISCUSSION

3.1 Characterization of Au@Pt NPs

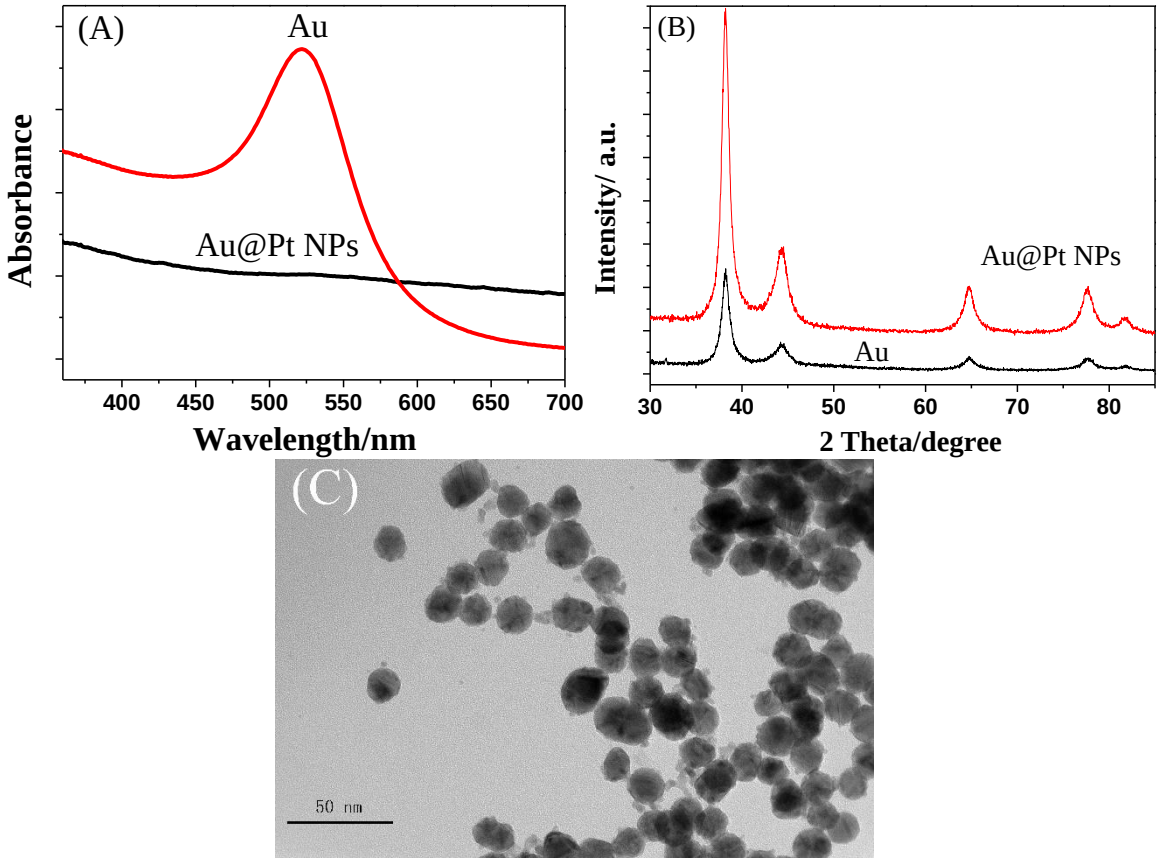

Figure 1. (A) UV-vis spectra of Au and Au@Pt NPs. (B) XRD of Au and Au@Pt NPs. (C) TEM of Au@Pt NPs

From Fig. 1(A), a strong absorption peak around 520 nm responded to Au seeds, while the absorption peak at 520 nm had disappeared completely in Au@Pt NPs. The results indicated that Pt shell has been coated on the Au core and the optical property has been dominated by Pt, implying that Au @ Pt NPs has been successfully synthesized. The comparisons of XRD between Au and Au@Pt NPs were displayed in Fig. 1(B). The diffraction angles (2θ) of 38.24°, 44.58°, 64.74° and 77.70° were responded to the diffraction peaks of (111), (200), (220) and (311) crystal faces of Au nanoparticles, respectively. However, the diffraction peaks angles (2θ) of Au@Pt NPs appeared at 38.29°, 44.46°, 64.65° and 77.70°, indicating that Pt nanoparticles have been successfully loaded on the Au nanoparticle [20]. Compared with the Au nanoparticle, the 2θ of (111), (200), (220) and (311) facets of Au@Pt NRs change little (< 0.12°), which result from the discrepancy of atom weight and the electron density between Au and Pt. These results indicated that there has a good crystallization of Au@Pt NRs. In addition, the TEM of Au@Pt NPs (Fig. 1(C)) showed that the nanoparticles maintain a similar spherical morphology with an average diameter of ~17.0 nm. The Au@Pt NPs possessed the obvious core-shell structure with Au as a core and Pt as a shell. It can be assumed that the synthesis of Au@Pt NPs was found to follow “seeded growth” mechanism, as reported by Hoefelmeyer et al [21].

3.2 Characterization of N-doped graphene (NG)

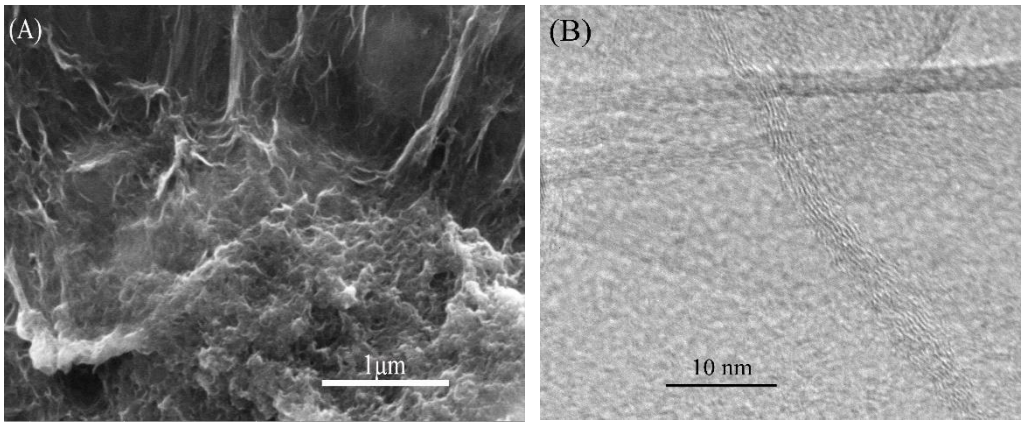

Figure 2. SEM (A) and TEM (B) image of NG

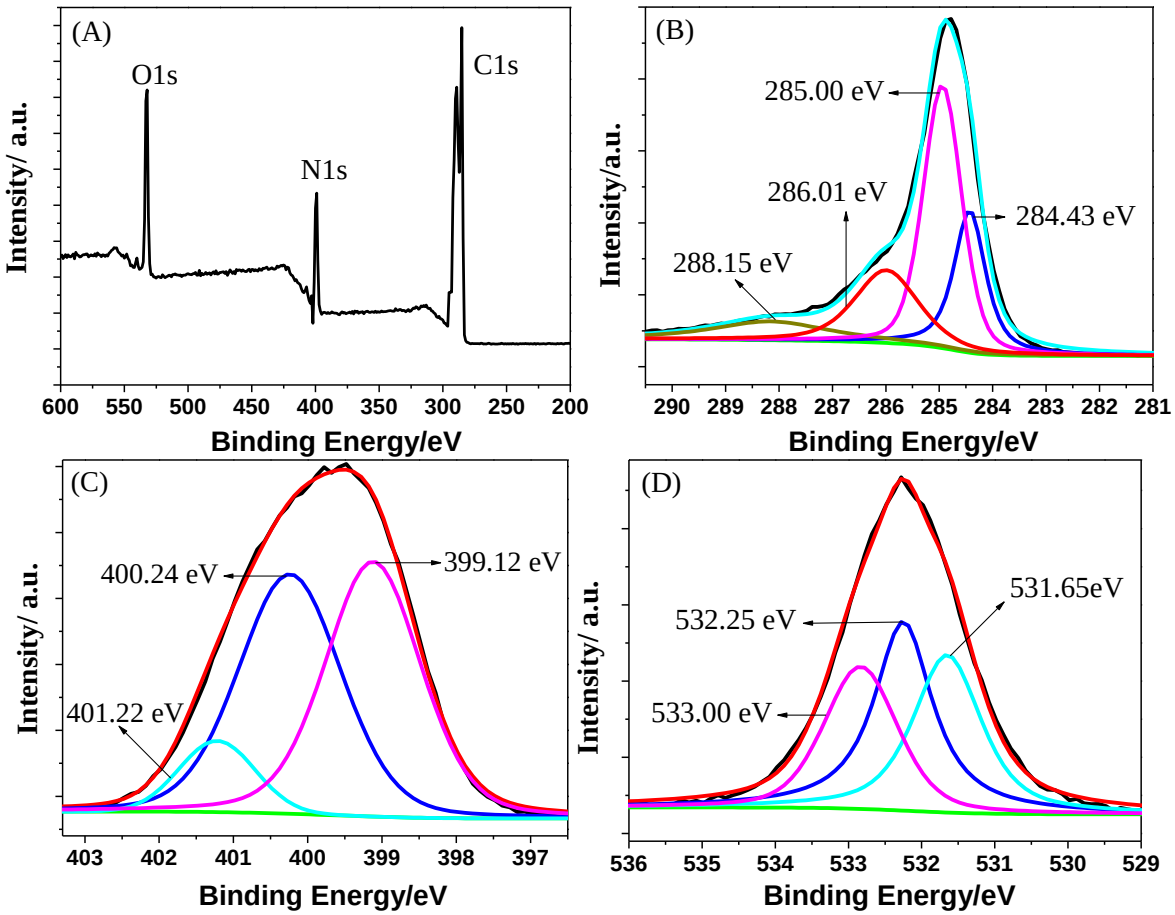

Figure 3. (A) XPS survey spectrum of NG. (B) XPS spectrum of C1s. (C) XPS spectrum of N1s. (D) XPS spectrum of O1s.

The SEM and TEM of the as-synthesized NG were investigated to obtain morphology and the results were shown in Fig. 2. It can be found that the agglomerated individual layers stacked together and formed sheet-like of graphene nanosheets with folded structure (Fig. 2(A)). The NG presented transparent, disorderly and wrinkled sheets (Fig. 2(B)), suggesting that N doping has not changed the

3D structure and crumpled-like surface of the grapheme, which can greatly facilitate electron transfer and the access of analyte [22].

XPS was used to identify the element components and the nature of the binding between carbon and nitrogen, as shown in Fig. 3. The XPS spectrum of NG showed three obvious peaks (Fig. 3. (A)), C1s (285.08 eV), N1s (402.08 eV) and O1s (531.08 eV), indicating that nitrogen atoms have already been bonded to carbon atoms. In addition, the abundant nitrogen and oxygen groups would result in excellent hydrophilicity, which was beneficial for the construction of electrochemical sensor. From Fig. 3(B), four fitting peaks with binding energies of 284.43 eV, 285.00 eV, 286.01 eV and 288.15 eV were attributed to C=C, C-C/C-N, C-O and -COOH, respectively [23]. The peaks at 399.12 eV, 400.24 eV and 401.22 eV in high-resolution N1s XPS spectra (Fig. 3(C)) referred to pyridinic N, pyrrolic N and graphitic N, respectively, consistent with the documents [23]. Fig. 3(D) showed three distinguishable peaks of C=O-OH (531.65 eV), C-O (532.25 eV) and C-OH (533.00 eV), respectively [22].

3.3 Characterization of NG-Au@Pt NPs

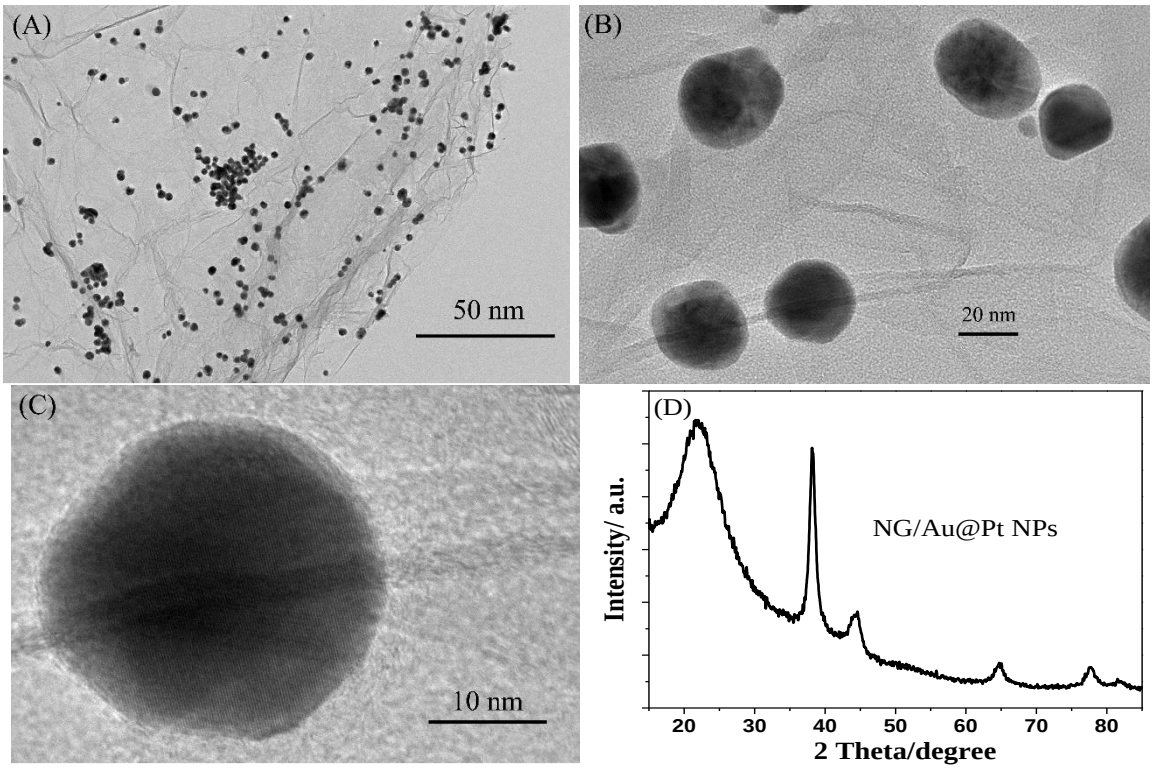

Figure 4. TEM images of NG-Au@Pt NPs at different magnification (A, B and C). (D) XRD patterns of NG-Au@Pt NPs

To investigate the structure and morphology of NG-Au@Pt NPs, TEM images at different magnification were obtained and shown in Fig. 4. The TEM images of NG-Au@Pt NPs (Fig. 4(A) and 4(B)) showed that the NG-Au@Pt NPs were uniformly dispersed on the transparent NG sheets. Furthermore, the free Au@Pt NPs can hardly be found outside the NG sheets, implying that plenty of

Au@Pt NPs had anchored on the surface of NG evenly. The NG-Au@Pt NPs still present wrinkled sheets on the surface and maintain a similar spherical morphology with an average diameter of ~22.0 nm, as shown in Fig. 4(B) and 4(C). XRD has been adopted for the determination of the phase composition of NG-Au@Pt NPs and was shown in Fig. 4(D). The obvious diffraction peak located at 2θ = 21.62° was attributed to the graphene sheets of (002) plane [13, 24, 25]. The diffraction angles (2θ) of 38.29°、44.46°、64.65° and 81.36° were originated from the diffraction peaks of (111), (200), (220) and (311) crystal faces of NG-Au@Pt NPs, respectively, responding to the phases of both Au and Pt diffractions [24, 26]. XRD results demonstrated that NG-Au@Pt NPs were composed of Au, Pt and NG elements.

3.4 Electrochemical Characterization

3.4.1 Electrochemical behavior of catechin

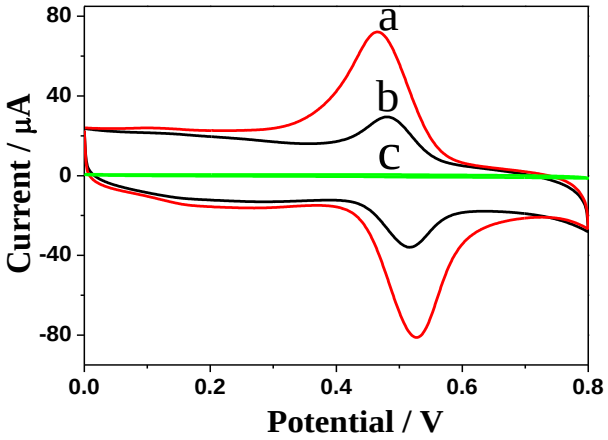

Figure 5. CVs of NG-Au@Pt NPs/ Au electrode (a), NG/Au electrode (b), bare Au electrode (c) in the 45 μM catechin solution, 20 mL PBS (pH = 2.2), scan rate of 50 mV/s.

The voltammetric responses of NG-Au@Pt NPs/Au electrode, NG/Au electrode and bare Au electrode toward determination of catechin with CV were compared (Fig. 5). It was clearly that the current at the bare Au electrode (curve c) nearly tended to zero, demonstrating that zero response with catechin. However, rather high redox signals of catechin were obtained on NG-Au@Pt NPs/Au electrode (curve a) and NG/Au electrode (curve b), the probable reason being that the electrons on graphene were redistributed and produced many active sites after N doping, which result in excellent electrochemical activity [27]. In addition, the peak current of NG-Au@Pt NPs/Au electrode (curve a) was the highest one, indicating that it was NG-Au@Pt NPs with high sensitivity that has superior electro-activity to determinate catechin.

3.4.2 Optimization of experimental conditions

3.4.2.1 Effect of the accumulation time and accumulation potential

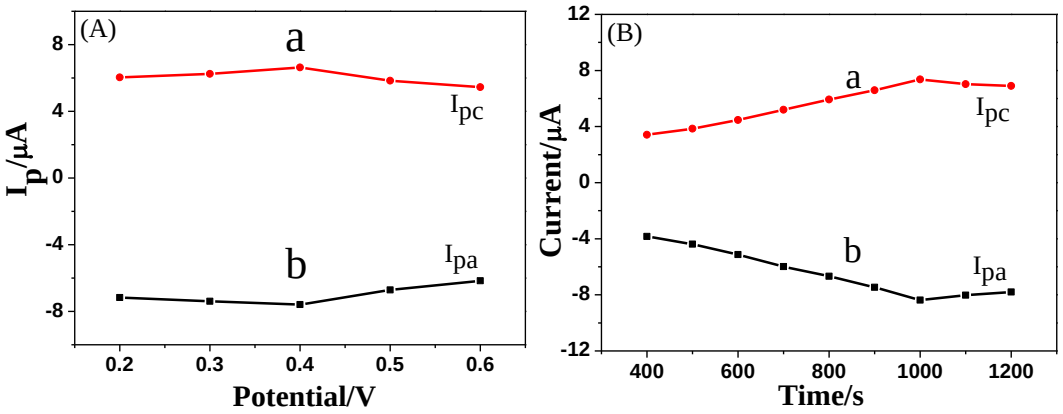

Figure 6. The effect of accumulation potential (A) and accumulation time (B) on the peak current of 45 μM catechin (0.20 M PBS (pH = 2.2))

The effect of accumulation potential and accumulation time on the determination of 45 μM catechin in 0.20 M PBS (pH = 2.2) has been investigated, and the results were shown in Fig. 6. The anode (I_{pa}) and cathode (I_{pc}) peak currents of catechin increased gradually with accumulation potential and reached maximum at 0.4 V (Fig. 6(A)), demonstrating that 0.4 V was adequate saturation of catechin on NG-Au@Pt NPs/Au electrode. Similarly, the I_{pa} and I_{pc} peak currents of catechin increased obviously with the incubation time increasing before 1000 s and then decreased gradually as the incubation time increased further (Fig. 6(B)), demonstrating that the adsorption equilibrium can be attained after 1000 s. Therefore, 1000 s was adopted optimum for catechin analysis.

3.4.2.2 Influence of pH

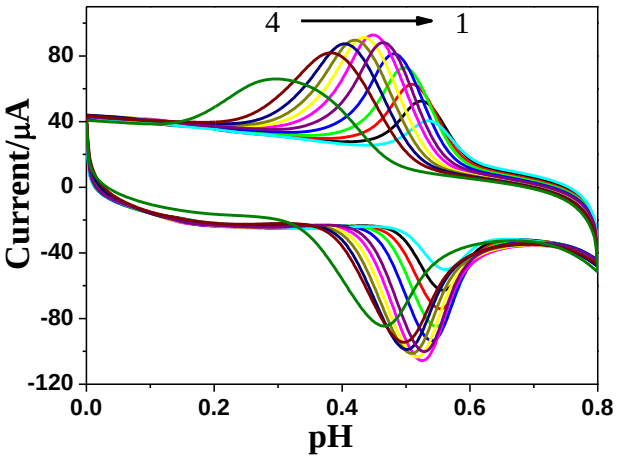

Figure 7. CVs of NG-Au@Pt NPs/Au electrode in PBS with different pH values (1, 1.2, 1.4, 1.6, 1.8, 2, 2.2, 2.4, 2.6, 2.8, 3 and 4), 45 μM catechin, scan rate of 50 mV/s.

The effect of different pH ranging from 1.0 to 4.0 on the electrochemical response of 45 μM catechin on NG-Au@Pt NPs/Au electrode was investigated. As can be seen from Fig. 7, the peak currents increased slightly with the increasing of pH and reached to the maximum value at pH = 2.2, and decreased gradually with the further increase of pH value. Therefore, to sensitively detect catechin, 2.2 of pH value was chosen in further experiments.

3.4.2.3 Effect of scan rate

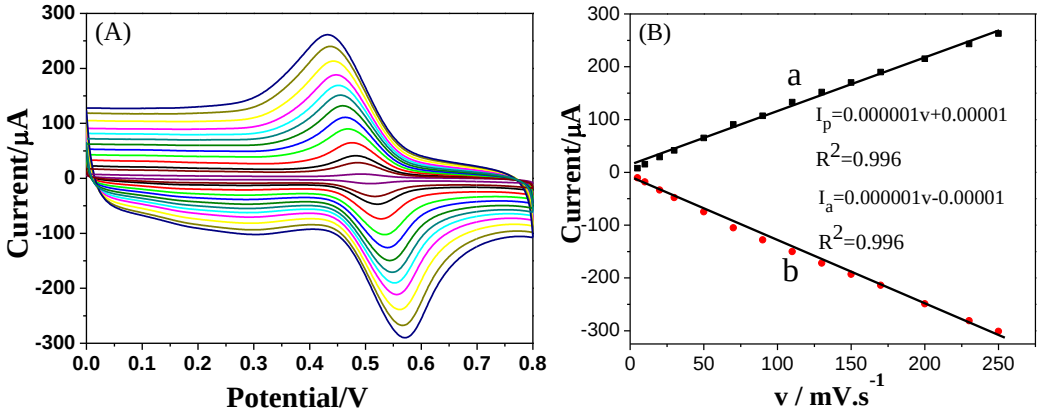

Figure 8. (A) CVs of NG-Au@Pt NPs/Au electrode. 45 μM catechin, pH=2.2, scan rate: 5, 10, 20, 30, 50, 70, 90, 110, 130, 150, 170, 200, 230, 250 mV/s). (B) Linear relationship of cathodic and anodic peak current versus vs. scan rate.

CVs of catechin were testes at different scan rates to investigate the electrochemical behavior of NG-Au@Pt NPs/Au electrode and the results were shown in Fig. 8. With rising scan rate from 5 to 250 mV/s, the increasing peak currents and the enlargement of the peaks distance were obtained (Fig. 8(A)), indicating that the electrode reaction gradually became more irreversible [24]. The linear relationship was observed between I_{pa} and I_{pc} peak currents and the scan rate in the range of 5-250 mV/s (Fig. 8(B)), demonstrating a quasi-reversible process with surface adsorption [28].

3.4.3 Determination of catechin

In this study, DPV has been used to study the sensitivity for determination of catechin due to its excellent sensitivity than CV, and the results were shown in Fig. 9 (A). The peak current was linear to the catechin concentration at NG-Au@Pt NPs/Au electrode in the range of 0.01-4.5×10^{-5} M. The regression equation was: I_p=350.73c (mM) + 26.615 (R^2=0.996) Fig. 9 (B), and the detection limits was 2.85×10^{-10} M (S/N=3). Experimental results implied that catechin can be successfully determined using NG-Au@Pt NPs/Au electrode. The comparison of similar electrodes and NG-Au@Pt NPs/Au electrode for catechin detection was shown in Table 1.

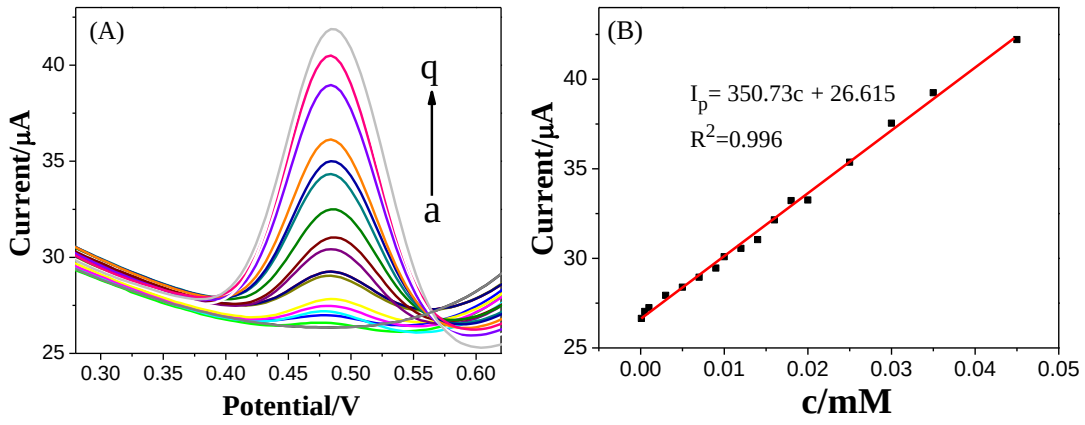

Figure 9. (A) DPV at NG-Au@Pt NPs/Au electrode in 0.20 M PBS (pH=2.2). Catechin concentrations: 1×10^{-7} M, 5×10^{-7} M, 1×10^{-6} M, 3×10^{-6} M, 5×10^{-6} M, 7×10^{-6}M, 9×10^{-6}M, 1×10^{-5} M, 1.2×10^{-5}M, 1.4×10^{-5}M, 1.6×10^{-5}M, 1.8×10^{-5} M, 2×10^{-5}M, 2.5×10^{-5} M, 3×10^{-5} M, 3.5×10^{-5} M, 4.5×10^{-5}M. (B) The relationship of I_p with catechin concentration.

Table 1. Comparison of similar electrodes and NG-Au@Pt NPs/Au electrode for catechin detection

Electrodes	Linear range	Detection limit	Reference
SWNTs-CTAB/GCE	3.72×10^{-10}-2.38×10^{-9} M	1.12×10^{-10} M	[11]
HP-β-CD	7.20-4.20 g·mL^{-1}	0.12-0.30 g·mL^{-1}	[14]
Laccase-modified electrode	4-40 μM	4.36 μM	[15]
Lac/CTS-g-N-CSIDZ-4-MBA@GNP/GD	8.7-146.0 μM	2.5 μM	[29]
NG-Au@Pt NPs/Au electrode	1.0×10^{-7}-4.5×10^{-5} M	2.85×10^{-9} M.	This work

3.4.5 Stability of the Au@AuPt NPs/Au electrode

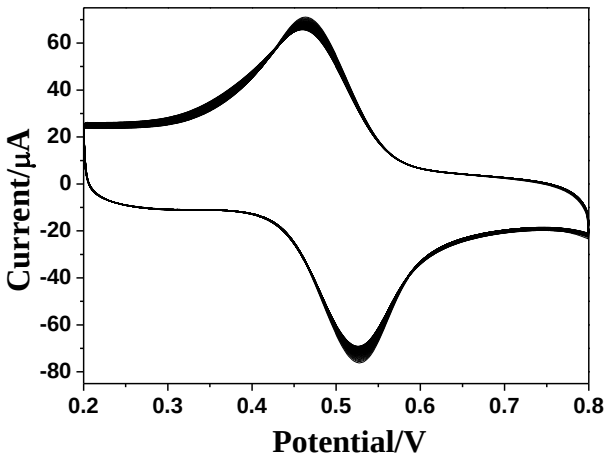

Figure 10. CVs of catechin electrocatalytic reaction at the NG-Au@Pt NPs/Au electrode in 0.20 M PBS (pH = 2.2) containing 45 μM catechin for 60 consecutive cycles.

In order to investigate the stability, NG-Au@Pt NPs/Au electrode was scanned continuously for 60 cycles at a scan rate of 50 mV/s. The features of the CVs were no obvious differences after 60 cycles (Fig. 10), demonstrating the excellent stability of NG-Au@Pt NPs/Au electrode. Therefore, the proposed NG-Au@Pt NPs/Au electrode could be employed for detection of catechin with high reproducibility and excellent stability, which result from the enhanced biocompatibility and catalytic activity of NG-Au@Pt NPs.

3.4.6 Sample analysis

Table 2. Results of catechin detection in Pu'er tea samples (n=3).

Sample	Original (μM)	Added (μM)	Found (μM)	Recovery (%)	RSD (%)
1	2.552	3	5.584	101.0	1.0
2	2.552	5	7.549	99.94	0.06
3	2.552	8	10.671	101.5	1.5

To evaluate the feasibility and applicability of the proposed method, Pu'er tea was selected as real sample and the concentration of catechin was detected. The Pu'er tea sample (0.05 g dry weight) added in 50 mL boiled water and heated for 10 min. Then, the residual solid was removed by filtering and the solution was diluted to 100 mL with PBS (pH = 2.2) to prepare the solution. Finally, DPV was employed for the determination of catechin, the recovery was 99.94-101.50 % and the RSD were 0.06-1.50 % (Table 2), which indicated that the proposed method is suitable for catechin determination in real tea samples.

4. CONCLUSIONS

In this paper, a hydrothermal method was employed to prepare N-doped grapheme (NG) with graphemes oxide (GO) as raw material, melamine ($C_3H_6N_6$) as reductant and nitrogen source. Then, Au@Pt core-shell nanoparticles (Au@Pt NPs) were embedded in NG to form hybrid nanocatalysts of N-doped Au@AuPt core-shell nanoparticles (NG-Au@Pt NPs). It was founded Au@Pt NPs had anchored on the surface of NG evenly and dispersed on the transparent NG sheets. The NG-Au@Pt NPs present wrinkled sheets on the surface and maintain a similar spherical morphology, and were composed of Au, Pt and NG elements. Significantly, the NG-Au@Pt NPs was dropped on Au electrode to obtain a modified gold electrode (NG-Au@Pt NPs/Au electrode), which has superior electro-activity to determinate catechin due to the increased active sites after N doping. Under the optical experimental condition, the electrochemical sensor for catechin exhibited a wide linear range of 1.0×10^{-7}-4.5×10^{-5} M and the detection limits was 2.85×10^{-10} M (S/N=3). The proposed method was successfully used to determination of catechin in tea samples with acceptable recovery range (97.23-101.65%) and RSD (0.06-1.5%).

ACKNOWLEDGMENTS
The authors gratefully acknowledge the financial support from the Yunnan education department of Scientific Research Foundation (2018JS478, 2019J1183), Yunnan Local Colleges Applied Basic Research Projects (2018FH001-114, 2018FH001-049 and 2017FD157) and the National Natural Science Foundation of China (51362012, 51662007 and 51574213)

References

1. H. Arakawa, M. Kanemitsu, N. Tajima, M. Maeda, *Anal. Chim. Acta*, 472 (2002) 75-82.
2. M.A. Hidayat, F. Jannah, B. Kuswandi, *Agric. Sci. Procedia*, 9 (2016) 424-430.
3. A. Dube, J.A. Nicolazzo, I. Larson, *Eur. J. Pharm. Sci.*, 41 (2010) 219-225.
4. I.C.W. Arts, P.C.H. Hollman, *J. Agric. Food Chem.*, 46 (1998) 5156-5162.
5. H.Y. Hsiao, R.L.C. Chen, T.J. Cheng, *Food Chem.*, 120 (2010) 632-636.
6. K. Dhalwal, V.M. Shinde, Y.S. Biradar, K.R. Mahadik, *J. Food Compos. Anal.*, 21 (2008) 496-500.
7. M. Bedner, D.L. Duewer, *Anal. Chem.*, 83 (2011) 6169-6176.
8. M. J. Skowron, A. Z. Grześkowiak, R. Frankowski, *J. Food Compos. Anal.*, 74 (2018) 71-81.
9. R. Song, Y. Cheng, Y. Tian, Z.-J. Zhang, *Chin. J. Nat. Medicines*, 10 (2012) 275-278.
10. T.T. Zhang, J.S. Zhou, Q. Wang, *Chin. J. Nat. Medicines*, 8 (2010) 107-113.
11. L.J. Yang, C. Tang, H.Y. Xiong, X.H. Zhang, S.F. Wang, *Bioelectrochemistry*, 75 (2009) 158-162.
12. R. Apak, S. Demirci Cekic, A. Cetinkaya, H. Filik, M. Hayvali, E. Kilic, *J. Agric. Food. Chem.*, 60 (2012) 2769-2777.
13. M. Meshki, M. Behpour, S. Masoum, *Anal. Biochem.*, 473 (2015) 80-88.
14. D.A. El-Hady, *Anal. Chim. Acta*, 593 (2007) 178-187.
15. A.J.Wilkołazka, T. Ruzgas, L. Gorton, *Enzyme Microb. Technol.*, 35 (2004) 238-241.
16. C.H. Zhang, L. Fu, N. Liu, M.H. Liu, Y.Y. Wang, Z.F. Liu, *Adv Mater.*, 23 (2011) 1020-1024.
17. P.V. Nidheesh, *Environ. Sci. Pollut. Res.*, 24 (2017) 27047-27069.
18. G. Frens, *Nat. Phys. Sci.*, 241 (1973) 20-22.
19. W.S. Jr, R.E. Offeman, *J. Am. Chem. Soc.*, 80 (1958).
20. I.S. Park, K.S. Lee, D.S. Jung, H.Y. Park, Y.E. Sung, *Electrochim. Acta*, 52 (2007) 5599-5605.
21. J.D. Hoefelmeyer, K. Niesz, G.A. Somorjai, T.D. Tilley, *Nano Lett.*, 5 (2005) 435-438.
22. X.L. Chen, G.W. Zhang, L. Shi, S.Q. Pan, W. Liu, H.B. Pan, *Mater. Sci. Eng. C*, 65 (2016) 80-89.
23. S.N. Wang, S. Liu, J.Y. Zhang, Y. Cao, *Talanta*, 198 (2019) 501-509.
24. X.L. Chen, G.M. Yang, S.P Feng, L. Shi, Z.L. Huang, H.B. Pan, W. Liu, *Appl. Surf. Sci.*, 402 (2017) 232-244.
25. H. K, R.P. Joshi, S. D.V, V.N. Bhoraskar, S.D. Dhole, *Appl. Surf. Sci.*, 389 (2016) 1050-1055.
26. F.Y. Kong, L. Yao, R.F. Li, H.Y. Li, Z.X. Wang, W.X. Lv, W. Wang, *J. Alloys Compd.*, 797 (2019) 413-420.
27. A. Salah, M. Hassan, J. Liu, M. Li, X. Bo, J.C. Ndamanisha, L. Guo, *J. Colloid Interface Sci.*, 512 (2018) 379-388.
28. R. Abdel-Hamid, E.F. Newair, *J. Electroanal. Chem.*, 704 (2013) 32-37.
29. Y. Yang, H. Zeng, Q. Zhang, X. Bai, C. Liu, Y.H. Zhang, *Chem. Phys. Lett.*, 658 (2016) 259-269.